HHS Public Access

Author manuscript

ACS Appl Mater Interfaces. Author manuscript; available in PMC 2018 April 06.

Published in final edited form as:

ACS Appl Mater Interfaces. 2016 October 19; 8(41): 27585–27593. doi:10.1021/acsami.6b09839.

Antifouling Electrospun Nanofiber Mats Functionalized with Polymer Zwitterions

Kristopher W. Kolewe[†,1], **Kerianne M. Dobosz**[†,1], **Katrina A. Rieger**[1], **Chia-Chih Chang**[2], **Todd Emrick**[2], and **Jessica D. Schiffman**[1,*]

[1]Department of Chemical Engineering, University of Massachusetts Amherst, Amherst, Massachusetts 01003-9303

[2]Department of Polymer Science and Engineering, University of Massachusetts Amherst, Massachusetts 01003-9303

Abstract

In this study, we exploit the excellent fouling resistance of polymer zwitterions and present electrospun nanofiber mats surface-functionalized with poly(2-methacryloyloxyethyl phosphorylcholine) (polyMPC). This zwitterionic polymer coating maximizes the accessibility of the zwitterion to effectively limit biofouling on nanofiber membranes. Two facile, scalable methods yielded a coating on a cellulose nanofiber platform: (i) a two-step sequential deposition featuring dopamine polymerization followed by the physioadsorption of polyMPC; and (ii) a one-step codeposition of polydopamine (PDA) with polyMPC. While the sequential and codeposited nanofiber mat assemblies have an equivalent average fiber diameter, hydrophilic contact angle, surface chemistry, and stability, the topography of nanofibers prepared by codeposition were smoother. Protein and microbial antifouling performance of the zwitterion modified nanofiber mats along with two controls, cellulose (unmodified) and PDA coated nanofiber mats were evaluated by dynamic protein fouling and prolonged bacteria exposure experiments. Following 21 days of exposure to bovine serum albumin, the sequential nanofiber mats significantly resisted protein fouling, as indicated by their 95% flux recovery ratio in a water flux experiment, 300% improvement over the cellulose nanofiber mats. When challenged with two model microbes *Escherichia coli* and *Staphylococcus aureus* for 24 hr, both zwitterion modifications demonstrated superior fouling resistance by statistically reducing microbial attachment over the two controls. This study demonstrates that by decorating the surfaces of chemically and mechanically robust cellulose nanofiber mats with polyMPC, we can generate high performance, free-standing nanofiber mats that hold potential in applications where antifouling materials are imperative, such as tissue engineering scaffolds and water purification technologies.

Graphical abstract

[*]Corresponding author: Jessica D. Schiffman, schiffman@ecs.umass.edu; Phone: (413) 545-6143.

[†]These authors contributed equally.

Supporting Information. The Supporting Information is available and free of charge http://pubs.acs.org.

Keywords

Antifouling; Dopamine; Electrospin; Nanofiber; Phosphorylcholine; Zwitterion

INTRODUCTION

Electrospinning is a scalable and versatile technique for producing highly porous materials that exhibit outstanding structure-property relationships.[1,2] The produced mats are comprised of nano- and macroscale diameter fibers, which have microscale interstitial spacing, a large surface-to-volume ratio, high specific surface area, and porosity values greater than >80%.[3,4] By coupling their unique structural characteristics with an optimized surface chemistry, electrospun fiber mats are promising for applications ranging from tissue engineering,[5,6] to wearable electronics,[7] to water purification technologies.[8,9] Unfortunately, these materials are susceptible to biofouling, which can cause detrimental complications, such as, reduced efficiency and selectivity of membranes[10] and infections from contaminated medical devices.[11]

Biofouling is characterized as a nonspecific surface attachment of biomolecules, microorganisms, and mammalian cells.[12,13] The initial adhesion of biomolecules and microbes can be delayed through manipulation of surface properties, *i.e.*, surface chemistry, surface topography, and mechanical properties.[14,15] Because of their enhanced stability and excellent fouling resistance, polymer zwitterions have emerged as a promising class of antifouling materials.[16,17] The charge-neutral zwitterionic moieties attract water to the surface forming a hydration layer[18,19] that is likely responsible for excellent protein adsorption resistance[20] and reduced bacterial adhesion.[21]

Electrospinning with zwitterions has been limited to sulfobetaine derivatives and the as-spun fibers were observed to lack chemical and/or mechanical integrity.[22] Brown *et al.*[23] demonstrated that zwitterionic copolymers containing sulfobetaine methacrylate in a poly(*n*-butyl acrylate) matrix could be electrospun into fibers of ~100 nm diameter. Due to the low solution concentration and viscosity, fiber spinning was hypothesized to result from zwitterion aggregation rather than chain entanglement. In contrast, it was demonstrated that a high solution concentration of high molecular weight poly(sulfobetaine methacrylate) favored smooth fiber formation with diameters ranging from 200 to 800 nm.[24,25] In a subsequent report, Lalani and Liu[26] used a three-step process, namely, polymerization, electrospinning, and photo-crosslinking, to form water-stable Ag^+ impregnated poly(sulfobetaine methacrylate) nanofiber mats that were antifouling and antibacterial. An

additional study incorporated sulfobetaine groups into small diameter tissue engineered vascular grafts by spinning biodegradable, elastic polyurethanes containing sulfobetaine from a polycaprolactone-diol:sulfobetaine-diol mixture reacted with diisocyanatobutane and chain-extended with putrescine.[27] Cyanoacrylate monomers (i.e., super glue), have been electrospun alone[28] and in combination with other acrylic polymers via air-flow assistance[29] and via the rapid polymerization of the ethyl-2-cyanoacrylate monomer in the presence of moisture.[30] While preliminary success at spinning zwitterion-containing solutions has been demonstrated, the solution and apparatus requirements, i.e., polymer concentration, solvent system, applied voltage, etc., must be re-optimized in each case. Additionally, after optimization, there is no guarantee that the zwitterion are present at the surface of the nanofiber mats for maximizing non-fouling effects. We suggest that a facile, effective nanofiber mat surface modification, which potentially could be employed for any polymer zwitterion, would represent a cost-effective approach towards controlling fouling while retaining the chemical stability and mechanical properties of the underlying nanofiber mat.[31–33]

Under alkaline conditions, bioinspired dopamine undergoes oxidative polymerization to yield surface-adherent, ultrathin, hydrophilic polydopamine (PDA) coatings.[34,35] However, after prolonged exposure to proteins and microorganisms, PDA coatings are prone to fouling,[36–38] making the inclusion of functional antifouling moieties a necessity to improve their performance. Conveniently, the chemical structure of PDA incorporates many functional groups, such as catechol, amine, and imine, which are amendable to covalent modification[35] using techniques common to antifouling applications,[39–41] including layer-by-layer assembly,[42] polymer grafting,[43,44] and peptide immobilization.[37] In terms of zwitterion incorporation, our group[38] and Zhou *et al.*[45] have demonstrated that polymer zwitterion can be immobilized using a codeposition method with PDA to form an ultrathin composite coating on a variety of surfaces, including, silicon, glass, polystyrene, perfluorinated silicon, steel, and microporous polypropylene membranes.

In this work, we investigate codeposition, as well as a sequential modification method that directly functionalizes the surface of electrospun nanofiber mats with the polymer zwitterion poly(2-methacryloyloxyethyl phosphorylcholine) (polyMPC).[46] These techniques are intended to maximize the accessibility and functionality on the fiber surface. We selected cellulose nanofibers as the platform base material, as this biopolymer represents an abundant source of biomedical and environmental materials.[47] Our previous work examined polyMPC/PDA codeposition kinetics, surface roughness, surface composition, and coating stability to determine the optimal concentration and conditions to control coating thickness and surface roughness on flat, non-porous substrates.[38] Here, we employ polyMPC/PDA in a codeposition and sequential coating method to functionalize nanofibers. The surface topography, chemistry, protein fouling, and microbial fouling of the four hydrophilic nanofiber mats, cellulose (control), PDA-functionalized, and polymer zwitterion functionalized (via codeposition and sequential methods) were evaluated. To our knowledge, this represents the first use of polymer zwitterions directly on the surface of nanofiber mats. As will be described, we find that a facile surface functionalization imparts significant antifouling properties without sacrificing the inherent porous architecture, mechanical, or chemical stability of the underlying nanofiber mat.

MATERIALS AND METHODS

Materials and Chemicals

All compounds were used as received. Cellulose acetate (M_w = 30 kDa), dopamine hydrochloride, M9 minimal salts (M9 media), D-(+)-glucose, calcium chloride (anhydrous), phosphate buffered saline (PBS, 1 × sterile biograde), Luria-Bertani broth (LB) tryptic soy broth (TSB), bovine serum albumin (BSA, M_w = ~66 kDa), and sodium chloride (NaCl) were obtained from Sigma-Aldrich (St. Louis, MO). Tris(hydroxymethyl)aminomethane (Tris), ethanol, and sodium hydroxide (NaOH) were obtained from Fisher Scientific (Fair Lawn, NJ). Deionized (DI) water was obtained from a Barnstead Nanopure Infinity water purification system (Thermo Fisher Scientific, Waltham, MA).

Fabrication of Cellulose Nanofiber Mats

A 15 w/v% solution of cellulose acetate in acetone was mixed for 24 hr at 20 rpm using an Arma-Rotator A-1 (Bethesda, MA).[48] The solution was loaded into a 5 mL Luer-Lock tip syringe capped with a Precision Glide 18-gauge needle (Becton, Dickinson & Co. Franklin Lakes, NJ), which was secured to a PHD Ultra syringe pump (Harvard Apparatus, Plymouth Meeting, PA). Alligator clips were used to connect the positive anode of a high-voltage supply (Gamma High Voltage Research Inc., Ormond Beach, FL) to the needle and the negative anode to a copper plate wrapped in aluminum foil. A constant feed rate of 3 mL/hr, an applied voltage of 25 kV, and a separation distance of 10 cm were used to spin cellulose acetate. The assembled electrospinning apparatus was housed in an environmental chamber (CleaTech, Santa Ana, CA) with a desiccant unit (Drierite, Xenia, OH) to maintain a temperature of 22 ± 1 °C and a relative humidity of 55%. All nanofiber mats used in this study were electrospun for 1 hr. To convert the cellulose acetate nanofibers to cellulose nanofibers, the mats were sandwiched between sheets of Teflon and thermally treated at 208 °C for 1 hr before being submerged in a 0.1 M NaOH 4:1 v/v of water/ethanol solution for 24 hr. The cellulose nanofiber mats were placed in a desiccator for 24 hr at room temperature (23 °C) before functionalization.

Preparation of PolyMPC/PDA Functionalized Nanofiber Mats

PolyMPC, Mn: 30 kDa, was prepared according to a previously published method.[38,49] The fabricated cellulose nanofiber mats were surface-functionalized using one of three following techniques: (i) only polydopamine (PDA), (ii) a sequential process using PDA then polyPMC, or (iii) a simultaneous codeposition of PDA and PMPC. First, the base platform cellulose nanofiber mats were punched into circles with 2.54 cm (1 inch) diameters using a Spearhead® 130 Power Punch MAXiset (Fluid Sealing Services, Wausau, WI) and placed in a 6-well plate with 5 mL of the desired functionalization solution. For PDA functionalization, the cellulose nanofiber mats were submerged in a freshly prepared Tris buffer (10 mM, pH 8.5) containing 2 mg/mL PDA for 6 hr.[35] For the sequentially functionalized nanofibers, the mats were submerged in the described PDA solution, then submerged in Tris buffer containing 2 mg/mL polyMPC for 24 hr.[38] Codeposition of PDA/polyMPC onto the nanofiber mats was achieved by submerging the mats in Tris buffer containing 2 mg/mL of PDA and 2 mg/mL polyMPC for 6 hr.[38] After each treatment, the

mats were rinsed 3× with DI water. Throughout this manuscript, we will refer to the three sample types as PDA, polyMPC/PDA sequential, and polyMPC/PDA codeposited.

Characterization of PolyMPC/PDA Functionalized Nanofiber Mats

Micrographs of cellulose nanofiber mats with and without functionalization (PDA, sequential, and codeposited) were acquired using an FEI-Magellan 400 scanning electron microscope (SEM, Hillsboro, OR). A Cressington 208 HR sputter coater (Cressigton Scientific Instruments, Watford, England) was used to coat samples with ~5 nm of platinum. The fiber diameter and particle diameter distribution were determined by measuring 50 random fibers or 100 random particles from 5 micrographs using *Image J1.45* software (National Institutes of Health, Bethesda, MD). A PerkinElmer Spectrum 100 Fourier transform infrared spectrometer (FTIR, Waltham, MA) confirmed the regeneration of cellulose acetate nanofiber mats to cellulose after the alkaline treatment. High resolution x-ray photoelectron spectroscopy (XPS, Physical Electronics Quantum 2000 Microprobe, Physical Electronics Inc., Chanhassen, MN) scans were obtained to determine the chemical composition using the known sensitivity factors. A monochromatic Al X-rays at 50 W was used with a spot area of 200 μm and the take-off angle was set to 45°. Contact angle measurements were acquired using a home-built apparatus equipped with a Nikon D5100 digital camera with a 60 mm lens and 68 mm extension tube (Nikon, Melville, NY).[50] Data represents the average of five drops of glycerol (4 μL) measured on two different cellulose, PDA, polyMPC/PDA sequential, and polyMPC/PDA codeposited nanofiber mats.

Dynamic Protein Fouling of PolyMPC/PDA Functionalized Nanofiber Mats

Free-standing cellulose nanofiber mats, with and without functionalization, were prepared to evaluate their fouling properties. Non-supported nanofiber mats were loaded into a 25 mm Sterlitech stirred-cell (Kent, WA) after being pre-wet using DI water for 12 hr. The mats were 76.2 ± 5 μm thick, as measured using a Mitutoyo 293–330 digital micrometer (Ontario, Canada) with an effective mat area of 3.80 cm^2. The initial pure water flux, $J_{w,i}$, was determined using Equation 1, where $V_{DI\ water}$ is the volume of water permeated through the membrane, Δt is the change time, and A_{mat} is the area of the mat. DI water was passed through the nanofiber mats at an applied pressure of 2 psi[51] with a stir rate of 600 rpm. The time was recorded for each 100 g of DI water that permeated through the nanofiber mat.

$$J_{w,i}\left(\frac{L}{m^2 h}\right) = \frac{V_{DI\ water}}{A_{mat} \times \Delta t} \quad \text{(Equation 1)}$$

$$J_{BSA}\left(\frac{L}{m^2 h}\right) = \frac{V_{BSA\ solution}}{A_{mat} \times \Delta t} \quad \text{(Equation 2)}$$

$$J_{w,f}\left(\frac{L}{m^2 h}\right) = \frac{V_{DI\ water}}{A_{mat} \times \Delta t} \quad \text{(Equation 3)}$$

$$FRR(\%) = \frac{J_{w,f}}{J_{w,i}} \times 100 \quad \text{(Equation 4)}$$

A BSA solution (250 mg/L in DI water) was used as a model fouling agent to find the permeation flux, J_{BSA}, Equation 2. The BSA solution (80 mL, pH 5.5) was passed through the nanofiber mats at an applied pressure of 4 psi.[51] After BSA testing, the non-rinsed nanofiber mats were submerged in 5 mL of DI water for 21 days to observe the long term BSA fouling. Samples were kept on a shaker plate at 75 rpm; the shaker prevents the nanofiber mat from settling in the well. Pure water flux of the nanofiber mats after BSA fouling and aging ($J_{w,f}$) was measured at an applied pressure of 2 psi. The flux recovery ratio (FRR) was calculated using Equation 4[52] and is a measure of membrane fouling resistance. All nanofiber mats were tested in triplicate. Significant differences between samples were determined with an unpaired student *t*-test. Significance ($p \leq 0.01$) is denoted in graphs by one (*) asterisk.

Bacterial Fouling of PolyMPC/PDA Functionalized Nanofiber Mats

The model gram-negative and gram-positive microorganisms were *Escherichia coli K12* MG1655 (*E. coli*) and *Staphylococcus aureus* SH1000 (*S. aureus*), respectively. *E. coli* purchased from DSMZ (Leibniz-Institut, Germany) contained a GFP plasmid while the *S. aureus* contained a high-efficiency pCM29 sGFP plasmid.[53] Free-standing cellulose nanofiber mats with and without functionalization (PDA, sequential, and codeposition), were punched into circles with 2.54 cm diameters and placed at the base of 6-well plates (Fisher Scientific) to which 5 mL of M9 media with 100 μg/mL ampicillin or 10 μg/mL chloramphenicol was added for *E. coli* or *S. aureus* (1.00×10^8 cells/mL), respectively. Internal controls (glass coverslips) were also run in parallel (data not shown). The growth media in each well was inoculated with an overnight culture of *E. coli* or *S. aureus*, which were washed and resuspended in M9 media,[54,55] then placed in an incubator at 37 °C for 24 hr. Nanofiber mats with attached bacteria were removed from the 6-well plates and washed with PBS to remove loosely adherent bacteria. *E. coli* and *S. aureus* attachment was evaluated using an adhesion assay[56,57] that monitored the bacteria colony coverage within a 366,964 μm^2 area using a Zeiss Microscope Axio Imager A2M (20× magnification, Thornwood, NY). The particle analysis function in *ImageJ* was used to calculate the bacteria colony area coverage (%) by analyzing 10–15 randomly acquired images over three parallel replicates. Significant differences between samples were determined with an unpaired student *t*-test. Significance ($p \leq 0.001$) is denoted in graphs by two (**) asterisks.

RESULTS AND DISCUSSION

Morphological Characteristics of PolyMPC/PDA Functionalized Nanofiber Mats

Cellulose nanofiber mats were successfully prepared by alkaline treatment of the electrospun cellulose acetate nanofiber mats, Figure 1. FTIR spectra of the as-spun cellulose acetate and the regenerated cellulose nanofiber mats are displayed in Figure S1 of the Supporting Information. Notably, the disappearance of the 1750 cm^{-1} peak indicates that the acetate groups have been replaced with hydroxyl groups supporting the regeneration of cellulose. Predominantly, the cellulose nanofiber mats displayed a cylindrical morphology[58,59] with an average fiber diameter of 1.08 ± 0.46 μm, Figure S1. The cellulose nanofiber mats served as the base substrate for the three surface functionalizations examined. Previous reports concluded that the thickness of PDA coatings can be reliably controlled by adjusting dopamine concentration, pH, temperature, buffer, and reaction time.[38,60–62] Since this study aims to explore the presentation of the zwitterionic moieties, we chose to use a consistent PDA coating condition that previously resulted in thin (~25 nm) underwater superoleophobic and antifouling coatings on silicon wafers.[38] As expected, stable coatings did not form on the cellulose nanofibers with polyMPC alone.

Visually, the as-prepared white cellulose nanofiber mats changed to brown after functionalization with PDA, polyMPC/PDA sequential, and polyMPC/PDA codeposition, consistent with previous reports.[63] Cellulose nanofiber mats that were coated with PDA exhibited particulate aggregates throughout the nanofiber matrix consistent with previous reports of PDA coatings on smooth surfaces.[60,61] The PDA particles within the aggregates had an average diameter of 0.73 ± 0.9 μm (Figure 2). Inspection of the SEM micrographs (Figure 1) showed that the polyMPC/PDA sequential deposition resulted in fewer large aggregates and decreased average particle size on the fiber surface (0.32 ± 0.3 μm). Notably, particle aggregation was nearly eliminated on the cellulose nanofiber mats that were functionalized using the one-step polyMPC/PDA codeposition method. Here, the surface of the individual nanofibers largely appeared smooth with average particle diameter of 0.14 ± 0.08 μm. Sundaram *et al.*[64] previously reported a similar finding, in the presence of a hydrophilic polymer, catechol-terminated poly(carboxybetaine methacrylate), reduced PDA aggregate size on microporous membranes from 3 μm to <100 nm. Overall, the average fiber diameter of the cellulose nanofiber mats functionalized with PDA, polyMPC/PDA sequential, and polyMPC/PDA codeposition, remained equivalent to the base cellulose nanofiber mats.

The effect of this surface functionalization on the hydrophilicity of the nanofiber mat was determined by static contact angle measurements using glycerol. Contact angles were determined to be statistically equivalent for all mats: 36.8 ± 6.7° for the unmodified cellulose nanofiber mats, 36.5 ± 6.2° for PDA, 34.0 ± 6.8° for polyMPC/PDA sequential, and 31.1 ± 5.3° for polyMPC/PDA codeposition. As expected, a hydrophilic contact angle was acquired on all nanofiber mats.

Chemical Characteristics of PolyMPC/PDA Functionalized Nanofiber Mats

Representative survey scans and high-resolution XPS spectra were acquired to determine the surface chemical composition of the cellulose, PDA and polyMPC/PDA nanofiber mats, Figure 3. Nitrogen signals were expectedly absent from the base cellulose nanofiber mats, while the PDA functionalized fibers exhibited a nitrogen signal at 399 eV, confirming successful PDA deposition.[61] Cellulose nanofiber mats functionalized with both PDA and polyMPC, either by sequential or codeposition method, were found to have a nearly identical surface composition of P_{2p} and N_{1s}, thus confirming the presence of polyMPC after their treatments (Figure 3 (B, C) and Table 1). Sequential and codeposited nanofiber mats displayed a characteristic phosphorus P_{2p} signal at 132.4 eV due to the presence of polyMPC, which was absent from the PDA functionalized materials. The phosphorus-to-carbon (P/C) ratio of the sequential and codeposited mats were 0.016 and 0.013, respectively, corresponding to 6.4 and 8.2 dopamine molecules for every PC group. The nitrogen N_{1s} region of the XPS spectra revealed a peak at 399 eV within the PDA functionalized nanofiber mats, indicative of primary amines. With the addition of polyMPC, a peak appears at 401 eV indicating the presence of quaternary amine that is unique to polyMPC. The spectra of the polyMPC/PDA sequential and codeposition nanofiber mats presented a 0.32 ± 0.1 and 0.36 ± 0.1 ratio of the quaternary amine to primary amine nitrogens.

Protein Antifouling Activity of PolyMPC/PDA Functionalized Nanofiber Mats

A dynamic protein fouling test was conducted on the cellulose nanofiber mats as well as the PDA and polyMPC/PDA functionalized mats using pure water and BSA solutions. As observed in Figure 4A, all nanofiber mats had identical pure water flux, with a final flux value of ~32,000 L m^{-2} h^{-1}, similar to a result previously reported.[22] Flux variability was observed to decrease as the test progressed, after ~2000 g of permeate passed through the mats, likely resulting from nanofiber compaction.[22,65] Despite the reported difference in particle aggregate size (Figure 2), the similar flux behavior between the cellulose and functionalized nanofiber mats might result from the large void space in the mats relative to the challenge molecules.

The fouling resistance of nanofiber mats was evaluated by measuring the pure water flux, $J_{w,f}$, of the fouled nanofiber mats following 21 days exposure to BSA. Figure 4B displays the calculated FRR value, which is a measure of the fouling resistance nature of a membrane calculated using Equation 4. In comparison to the non-functionalized cellulose nanofiber mats, the PDA, polyMPC/PDA sequential, and polyMPC/PDA codeposition nanofiber mats, all had a statistically significant increase in FRR values, 200%, 300%, and 150%, indicating their heightened fouling resistance over the cellulose nanofiber mats. The polyMPC/PDA sequential nanofiber mats exhibited a 98 ± 6% FRR, which was greater than the 80% FRR reported by Zhou *et al.*[45] who codeposited dopamine with poly(sulfobetaine methacrylate) on microporous microfiltration membranes.[8] Given that the pristine zwitterion-functionalized nanofiber mats had the same chemistry, hydrophilicity, and only a different topography, the better performance by the sequential nanofiber mats over the codeposited nanofiber mats was surprising and led us to investigate the stability of the coating.

Visually, the color change of the nanofiber mats persisted after the flux experiments and aging the samples for 21 days. SEM micrographs confirmed that the fiber morphology persisted as did the aggregates on the fiber surface, Figure S2. Additionally, XPS spectra acquired on samples following the flux experiments confirmed that the elemental composition of the nanofiber mats remained unchanged (Figure S3). Given these results, potentially, the physisorption of polyMPC to PDA-coated nanofiber mats provides the strongest BSA fouling resistance due to the presence of the zwitterion. Notably, independent of fiber chemistry, the mean void size of electrospun mats has been reported to be 3 ± 1 times the mean fiber diameter.[66] In this work, the cellulose nanofibers are ~1 μm in diameter and by accounting for the presence of the largest PDA particles (~0.7 μm), we estimate a ~4 to 7 μm void size, which is much larger than the size of pure water and the BSA foulant (hydrodynamic diameter of 6.8 nm).[67] However, since protein resistivity alone provides an incomplete view of the antifouling performance of materials, we further investigated the interactions of the nanofiber mats with microorganisms.

Bacterial Antifouling Activity of PolyMPC/PDA Functionalized Nanofiber Mats

The bacterial antifouling capability of the cellulose and polyMPC/PDA functionalized nanofiber mats was evaluated after 24 hr using two model microbes, the Gram-negative *E. coli* and the Gram-positive *S. aureus*. The extent of fouling from both microbes used in this study is observed visually by the representative florescence micrographs provided in Figure 5. Quantitatively, the colony area coverage of both bacterial species on cellulose nanofiber mats were statistically the same, 6.1 ± 0.5% and 6.3 ± 0.4% for *S. aureus* and *E. coli*, respectively. When cellulose nanofiber mats were functionalized with PDA, the amount of fouling by *S. aureus* increased to 7.5 ± 1.6% over the control cellulose nanofiber mats, while *E. coli* was unchanged, 6.3 ± 0.2%. Although PDA resists protein adsorption over short time periods, prolonged exposure leads to surface conditioning and ultimately bacterial fouling.[68] As demonstrated here, antifouling performance is improved markedly by incorporation of zwitterionic polymer.

The polyMPC/PDA sequential and codeposited coatings significantly reduced bacterial fouling of the nanofiber mats compared to PDA and cellulose controls. Sequential nanofiber mats reduced *S. aureus* fouling by 73% (2.0 ± 0.3%) relative to PDA and a statistically significant, 80% reduction in *E. coli* fouling (1.3 ± 0.2%). Codeposition generates a uniform coating that improved biofouling resistance by 79% and 85% compared to PDA, for *S. aureus (*1.6 ± 0.3%) and *E. coli* (1.0 ± 0.1%), respectively. The 85% fouling reduction achieved with the polyMPC/PDA coatings on high surface area nanofiber mats, is notably consistent to our previous demonstration on glass surfaces,[38] which is especially impressive considering the documented ability of 3D-scaffolds to readily adsorb bacteria.[48] These results indicate the presence of polyMPC on the surface of nanofibers significantly improves resistance to both protein and bacterial fouling, with some dependence on the deposition method. The adhesion of both bacterial species was ~25% greater on the polyMPC/PDA sequential nanofiber mats indicating the influence of a secondary effect, likely, surface morphology. The larger aggregates on the sequential nanofiber mats either promoted bacterial adhesion and/or the smoother surface of the codeposited coating prevented adhesion.

CONCLUSION

We have described the use of polyMPC as an antifouling coating on electrospun cellulose nanofiber mats using both a sequential and codeposited method featuring PDA. These composite materials hold potential for use in applications, such as, water treatment and wound healing where porous antibacterial materials are needed. Particle aggregate size was significantly reduced by polyMPC/PDA codeposition versus functionalizing the nanofiber mats with polyMPC/PDA sequential or PDA. While the initial pure water flux of all freestanding hydrophilic nanofiber mats was high, ~30,000 L m^{-2} h^{-1}, surface functionalization with polyMPC resulted in notable improvement after the nanofiber mats were fouled with BSA. The polyMPC/PDA nanofiber mats prepared by sequential coating exhibited the best results, with a 300% increase in FRR relative to the control cellulose nanofiber mats. We further investigated the ability of these mats to resist biofouling by challenging the mats with *E. coli* and *S. aureus* for 24 hr. Both functionalization methods showed significant improvement, yet codeposition performed noticeably better against both bacterial species (85% for *E. coli* and 79% for *S. aureus*). This may be due, at least in part to the morphology of the coating. Larger aggregates on the sequential coatings could provide adhesion points for bacterial attachment, but the exact mechanism is not yet understood. Nonetheless, this work indicates the utility of PDA as a robust bioinspired “glue” to maximize the efficiency of codeposited antifouling zwitterions, which we anticipate to be broadly applicable to efficiently limiting fouling on biomedical implants and membranes used for separations.

Supplementary Material

Refer to Web version on PubMed Central for supplementary material.

Acknowledgments

KWK was supported by National Research Service Award T32 GM008515 from the National Institutes of Health. This work was supported in part by a Fellowship from the University of Massachusetts to KMD as part of the Biotechnology Training Program (National Research Service Award T32 GM108556). TE acknowledges the support of the National Science Foundation (NSF CBET-1403742). This work was partially supported by the James M. Douglas Career Development Faculty Award and the Armstrong Fund for Science. Thanks to Dr. Michael Franklin (Montana State University) for kindly providing the florescence plasmid pMF 230 and to Dr. Alexander Horswill (University of Iowa) for the high-efficiency pCM29 sGFP plasmid. We thank Mr. Jack Hirsch for the assistance with XPS analysis. We acknowledge the use of facilities at the W.M. Keck Center for Electron Microscopy and the MRSEC at UMass Amherst.

References

1. Persano L, Camposeo A, Tekmen C, Pisignano D. Industrial Upscaling of Electrospinning and Applications of Polymer Nanofibers: A Review. Macromol Mater Eng. 2013; 298(5):504–520.
2. Gangwal S, Wright M. Nanofibres: New Scalable Technology Platform for Producing Polymeric Nanofibres. Filtr Sep. 2013; 50(2):30–33.
3. Deitzel J, Kleinmeyer J, Harris D, Beck Tan N. The Effect of Processing Variables on the Morphology of Electrospun Nanofibers and Textiles. Polymer. 2001; 42(1):261–272.
4. Moghadam BH, Haghi AK, Kasaei S, Hasanzadeh M. Computational-Based Approach for Predicting Porosity of Electrospun Nanofiber Mats Using Response Surface Methodology and Artificial Neural Network Methods. J Macromol Sci Part B Phys. 2015; 54(11):1404–1425.

5. Barnes CP, Sell SA, Boland ED, Simpson DG, Bowlin GL. Nanofiber Technology: Designing the next Generation of Tissue Engineering Scaffolds. Adv Drug Deliv Rev. 2007; 59(14):1413–1433. [PubMed: 17916396]
6. Wang X, Ding B, Li B. Biomimetic Electrospun Nanofibrous Structures for Tissue Engineering. Mater Today. 2013; 16(6):229–241.
7. Najafabadi AH, Tamayol A, Annabi N, Ochoa M, Mostafalu P, Akbari M, Nikkhah M, Rahimi R, Dokmeci MR, Sonkusale S, Ziaie B, Khademhosseini A. Biodegradable Nanofibrous Polymeric Substrates for Generating Elastic and Flexible Electronics. Adv Mater. 2014; 26(33):5823–5830. [PubMed: 25044366]
8. Lee J, Jung J, Cho YH, Yadav SK, Baek KY, Park HB, Hong SM, Koo CM. Fouling-Tolerant Nanofibrous Polymer Membranes for Water Treatment. ACS Appl Mater Interfaces. 2014; 6:14600–14607. [PubMed: 25116281]
9. Ma H, Hsiao BS, Chu B. Functionalized Electrospun Nanofibrous Microfiltration Membranes for Removal of Bacteria and Viruses. J Memb Sci. 2014; 452:446–452.
10. Baker JS, Dudley LY. Biofouling in Membrane Systems — A Review. Desalination. 1998; 118(1–3):81–89.
11. Costerton JW. Bacterial Biofilms: A Common Cause of Persistent Infections. Science. 1999; 284(5418):1318–1322. [PubMed: 10334980]
12. Flemming HC. Biofouling in Water Systems – Cases, Causes and Countermeasures. Appl Microbiol Biotechnol. 2002; 59(6):629–640. [PubMed: 12226718]
13. Flemming H-C, Wingender J. The Biofilm Matrix. Nat Rev Microbiol. 2010; 8(9):623–633. [PubMed: 20676145]
14. Banerjee I, Pangule RC, Kane RS. Antifouling Coatings: Recent Developments in the Design of Surfaces That Prevent Fouling by Proteins, Bacteria, and Marine Organisms. Adv Mater. 2011; 23(6):690–718. [PubMed: 20886559]
15. Magin CM, Cooper SP, Brennan AB. Non-Toxic Antifouling Strategies. Mater Today. 2010; 13(4): 36–44.
16. Holmlin RE, Chen X, Chapman RG, Takayama S, Whitesides GM. Zwitterionic SAMs That Resist Nonspecific Adsorption of Protein from Aqueous Buffer. Langmuir. 2001; 17(13):2841–2850.
17. Kane RS, Deschatelets P, Whitesides GM. Kosmotropes Form the Basis of Protein-Resistant Surfaces. Langmuir. 2003; 19(6):2388–2391.
18. Hower JC, Bernards MT, Chen S, Tsao HK, Sheng YJ, Jiang S. Hydration of “Nonfouling” functional Groups. J Phys Chem B. 2009; 113(1):197–201. [PubMed: 19072165]
19. White A, Jiang S. Local and Bulk Hydration of Zwitterionic Glycine and Its Analogues through Molecular Simulations. J Phys Chem B. 2011; 115:660–667. [PubMed: 21174438]
20. Tegoulia, Va; Rao, W; Kalambur, AT; Rabolt, JF; Cooper, SL. Surface Properties, Fibrinogen Adsorption, and Cellular Interactions of a Novel Phosphorylcholine-Containing Self-Assembled Monolayer on Gold. Langmuir. 2001; 17(14):4396–4404.
21. Kuang J, Messersmith PB. Universal Surface-Initiated Polymerization of Antifouling Zwitterionic Brushes Using a Mussel-Mimetic Peptide Initiator. Langmuir. 2012; 28(18):7258–7266. [PubMed: 22506651]
22. Huang L, Arena JT, Manickam SS, Jiang X, Willis BG, McCutcheon JR. Improved Mechanical Properties and Hydrophilicity of Electrospun Nanofiber Membranes for Filtration Applications by Dopamine Modification. J Memb Sci. 2014; 460:241–249.
23. Brown RH, Hunley MT, Allen MH, Long TE. Electrospinning Zwitterion-Containing Nanoscale Acrylic Fibers. Polymer. 2009; 50(20):4781–4787.
24. Lalani R, Liu L. Synthesis, Characterization, and Electrospinning of Zwitterionic Poly(sulfobetaine Methacrylate). Polymer. 2011; 52(23):5344–5354.
25. Emerick E, Grant S, Bernards M. Electrospinning of Sulfobetaine Methacrylate Nanofibers. Chem Eng Process Tech. 2013; 1003
26. Lalani R, Liu L. Electrospun Zwitterionic Poly(sulfobetaine Methacrylate) for Nonadherent, Superabsorbent, and Antimicrobial Wound Dressing Applications. Biomacromolecules. 2012; 13:1853–1863. [PubMed: 22545647]

27. Ye SH, Hong Y, Sakaguchi H, Shankarraman V, Luketich SK, DAmore A, Wagner WR. Nonthrombogenic, Biodegradable Elastomeric Polyurethanes with Variable Sulfobetaine Content. ACS Appl Mater Interfaces. 2014; 6(24):22796–22806. [PubMed: 25415875]
28. Mele E, Heredia-Guerrero JA, Bayer IS, Ciofani G, Genchi GG, Ceseracciu L, Davis A, Papadopoulou EL, Barthel MJ, Marini L, Ruffilli R, Athanassiou A. Zwitterionic Nanofibers of Super-Glue for Transparent and Biocompatible Multi-Purpose Coatings. Sci Rep. 2015; 5:14019. [PubMed: 26357936]
29. Jiang K, Long Y-Z, Chen Z-J, Liu S-L, Huang Y-Y, Jiang X, Huang Z-Q. Airflow-Directed in Situ Electrospinning of a Medical Glue of Cyanoacrylate for Rapid Hemostasis in Liver Resection. Nanoscale. 2014; 6(14):7792–7798. [PubMed: 24839123]
30. Liu S-L, Long Y-Z, Huang Y-Y, Zhang H-D, He H-W, Sun B, Sui Y-Q, Xia L-H. Solventless Electrospinning of Ultrathin Polycyanoacrylate Fibers. Polym Chem. 2013; 4(23):5696–5700.
31. Zhu J, Su Y, Zhao X, Li Y, Zhang R, Fan X, Ma Y, Liu Y, Jiang Z. Constructing a Zwitterionic Ultrafiltration Membrane Surface via Multisite Anchorage for Superior Long-Term Antifouling Properties. RSC Adv. 2015; 5(50):40126–40134.
32. Huang J, Wang D, Lu Y, Li M, Xu W. Surface Zwitterionically Functionalized PVA-Co-PE Nanofiber Materials by Click Chemistry. RSC Adv. 2013; 3(43):20922.
33. Huang C-J, Chu S-H, Wang L-C, Li C-H, Lee TR. Bioinspired Zwitterionic Surface Coatings with Robust Photostability and Fouling Resistance. ACS Appl Mater Interfaces. 2015; 7(42):23776–23786. [PubMed: 26452141]
34. Liu Y, Ai K, Lu L. Polydopamine and Its Derivative Materials: Synthesis and Promising Applications in Energy, Environmental, and Biomedical Fields. Chem Rev. 2014; 114(9):5057–5115. [PubMed: 24517847]
35. Lee H, Dellatore SM, Miller WM, Messersmith PB. Mussel-Inspired Surface Chemistry for Multifunctional Coatings. Science. 2007; 318(5849):426–430. [PubMed: 17947576]
36. Sileika TS, Kim HDo, Maniak P, Messersmith PB. Antibacterial Performance of Polydopamine-Modified Polymer Surfaces Containing Passive and Active Components. ACS Appl Mater Interfaces. 2011; 3(12):4602–4610. [PubMed: 22044029]
37. Cui J, Ju Y, Liang K, Ejima H, Lörcher S, Gause KT, Richardson JJ, Caruso F. Nanoscale Engineering of Low-Fouling Surfaces through Polydopamine Immobilisation of Zwitterionic Peptides. Soft Matter. 2014; 10(15):2656–2663. [PubMed: 24647351]
38. Chang C-C, Kolewe KW, Li Y, Kosif I, Freeman BD, Carter KR, Schiffman JD, Emrick T. Underwater Superoleophobic Surfaces Prepared from Polymer Zwitterion/Dopamine Composite Coatings. Adv Mater Interfaces. 2016; 3(6):521–530.
39. Decher G. Fuzzy Nanoassemblies: Toward Layered Polymeric Multicomposites. Science. 1997; 277(5330):1232–1237.
40. Zhai L, Cebeci FC, Cohen RE, Rubner MF. Stable Superhydrophobic Coatings from Polyelectrolyte Multilayers. Nano Lett. 2004; 4(7):1349–1353.
41. Kim HS, Ham HO, Son YJ, Messersmith PB, Yoo HS. Electrospun Catechol-Modified Poly(ethyleneglycol) Nanofibrous Mesh for Anti-Fouling Properties. J Mater Chem B. 2013; 1(32):3940–3949.
42. Pérez-Anes A, Gargouri M, Laure W, Van Den Berghe H, Courcot E, Sobocinski J, Tabary N, Chai F, Blach J-F, Addad A, Woisel P, Douroumis D, Martel B, Blanchemain N, Lyskawa J. Bioinspired Titanium Drug Eluting Platforms Based on a Poly-β-cyclodextrin–Chitosan Layer-by-Layer Self-Assembly Targeting Infections. ACS Appl Mater Interfaces. 2015; 7(23):12882–12893. [PubMed: 25992843]
43. Li Y, Su Y, Zhao X, He X, Zhang R, Zhao J, Fan X, Jiang Z. Antifouling, High-Flux Nanofiltration Membranes Enabled by Dual Functional Polydopamine. ACS Appl Mater Interfaces. 2014; 6(8):5548–5557. [PubMed: 24694079]
44. Jiang J, Zhu L, Zhu L, Zhang H, Zhu B, Xu Y. Antifouling and Antimicrobial Polymer Membranes Based on Bioinspired Polydopamine and Strong Hydrogen-Bonded Poly(n -Vinyl Pyrrolidone). ACS Appl Mater Interfaces. 2013; 5(24):12895–12904. [PubMed: 24313803]
45. Zhou R, Ren PF, Yang HC, Xu ZK. Fabrication of Antifouling Membrane Surface by Poly(sulfobetaine Methacrylate)/polydopamine Co-Deposition. J Memb Sci. 2014; 466:18–25.

46. Schlenoff JB. Zwitteration: Coating Surfaces with Zwitterionic Functionality to Reduce Nonspecific Adsorption. Langmuir. 2014; 30(32):9625–9636. [PubMed: 24754399]
47. Carpenter AW, de Lannoy C-F, Wiesner MR. Cellulose Nanomaterials in Water Treatment Technologies. Environ Sci Technol. 2015; 49(9):5277–5287. [PubMed: 25837659]
48. Rieger KA, Thyagarajan R, Hoen M, Yeung H, Ford D, Schiffman JD. Transport of Microorganisms into Cellulose Nanofiber Mats. RSC Adv. 2016; 6:24438–24445.
49. Bhuchar N, Deng Z, Ishihara K, Narain R. Detailed Study of the Reversible Addition–fragmentation Chain Transfer Polymerization and Co-Polymerization of 2-Methacryloyloxyethyl Phosphorylcholine. Polym Chem. 2011; 2(3):632–639.
50. Senbil N, He W, Démery V, Dinsmore AD. Effect of Interface Shape on Advancing and Receding Fluid-Contact Angles around Spherical Particles. Soft Matter. 2015; 11:4999–5003. [PubMed: 26001210]
51. Choong LTS, Lin YM, Rutledge GC. Separation of Oil-in-Water Emulsions Using Electrospun Fiber Membranes and Modeling of the Fouling Mechanism. J Memb Sci. 2015; 486:229–238.
52. Kim S-E, Zhang C, Advincula AA, Baer E, Pokorski JK. Protein and Bacterial Antifouling Behavior of Melt-Coextruded Nanofiber Mats. ACS Appl Mater Interfaces. 2016; 8(14):8928–8938. [PubMed: 27043205]
53. Pang YY, Schwartz J, Thoendel M, Ackermann LW, Horswill AR, Nauseef WM. Agr-Dependent Interactions of Staphylococcus Aureus USA300 with Human Polymorphonuclear Neutrophils. J Innate Immun. 2010; 2(6):546–559. [PubMed: 20829608]
54. Kolewe K, Peyton SR, Schiffman JD. Fewer Bacteria Adhere to Softer Hydrogels. ACS Appl Mater Interfaces. 2015; 7(35):19562–19569. [PubMed: 26291308]
55. Zodrow K, Schiffman J, Elimelech M. Biodegradable Polymer (PLGA) Coatings Featuring Cinnamaldehyde and Carvacrol Mitigate Biofilm Formation. Langmuir. 2012; 28(35):13993–13999. [PubMed: 22937881]
56. Fux, Ca; Wilson, S; Stoodley, P. Detachment Characteristics and Oxacillin Resistance of *Staphoccocus aureus* Biofilm Emboli in an In Vitro Catheter Infection Model. J Bacteriol. 2004; 186(14):4486–4491. [PubMed: 15231780]
57. Chung KK, Schumacher JF, Sampson EM, Burne Ra, Antonelli PJ, Brennan AB. Impact of Engineered Surface Microtopography on Biofilm Formation of *Staphylococcus aureus*. Biointerphases. 2007; 2(2):89–94. [PubMed: 20408641]
58. Ma Z, Kotaki M, Ramakrishna S. Electrospun Cellulose Nanofiber as Affinity Membrane. J Memb Sci. 2005; 265(1–2):115–123.
59. Frey MW. Electrospinning Cellulose and Cellulose Derivatives. Polym Rev. 2008; 48(2):378–391.
60. Della Vecchia NF, Luchini A, Napolitano A, D'Errico G, Vitiello G, Szekely N, d'Ischia M, Paduano L. Tris Buffer Modulates Polydopamine Growth, Aggregation, and Paramagnetic Properties. Langmuir. 2014; 30(30):9811–9818. [PubMed: 25066905]
61. Ding Y, Weng L-T, Yang M, Yang Z, Lu X, Huang N, Leng Y. Insights into the Aggregation/Deposition and Structure of a Polydopamine Film. Langmuir. 2014; 30(41):12258–12269. [PubMed: 25262750]
62. Xie J, Michael PL, Zhong S, Ma B, MacEwan MR, Lim CT. Mussel Inspired Protein-Mediated Surface Modification to Electrospun Fibers and Their Potential Biomedical Applications. J Biomed Mater Res – Part A. 2012; 100 A(4):929–938.
63. Yang H, Lan Y, Zhu W, Li W, Xu D, Cui J, Shen D, Li G. Polydopamine-Coated Nanofibrous Mats as a Versatile Platform for Producing Porous Functional Membranes. J Mater Chem. 2012; 22(33):16994–17001.
64. Sundaram HS, Han X, Nowinski AK, Brault ND, Li Y, Ella-Menye JR, Amoaka KA, Cook KE, Marek P, Senecal K, Jiang S. Achieving One-Step Surface Coating of Highly Hydrophilic Poly(Carboxybetaine Methacrylate) Polymers on Hydrophobic and Hydrophilic Surfaces. Adv Mater Interfaces. 2014; 1(6):1–8.
65. Huang L, Manickam SS, McCutcheon JR. Increasing Strength of Electrospun Nanofiber Membranes for Water Filtration Using Solvent Vapor. J Memb Sci. 2013; 436:213–220.
66. Ma H, Burger C, Hsiao BS, Chu B. Ultra-Fine Cellulose Nanofibers: New Nano-Scale Materials for Water Purification. J Mater Chem. 2011; 21(21):7507.

67. Fauchet PM. Charge- and Size-Based Separation of Maeromolecules Using Novel Ultrathin Silicon Membranes. Conf Proc – Lasers Electro-Optics Soc Annu Meet. 2007; 445:177.

68. Miller DJ, Araújo Pa, Correia PB, Ramsey MM, Kruithof JC, van Loosdrecht MCM, Freeman BD, Paul DR, Whiteley M, Vrouwenvelder JS. Short-Term Adhesion and Long-Term Biofouling Testing of Polydopamine and Poly(ethylene Glycol) Surface Modifications of Membranes and Feed Spacers for Biofouling Control. Water Res. 2012; 46(12):3737–3753. [PubMed: 22578432]

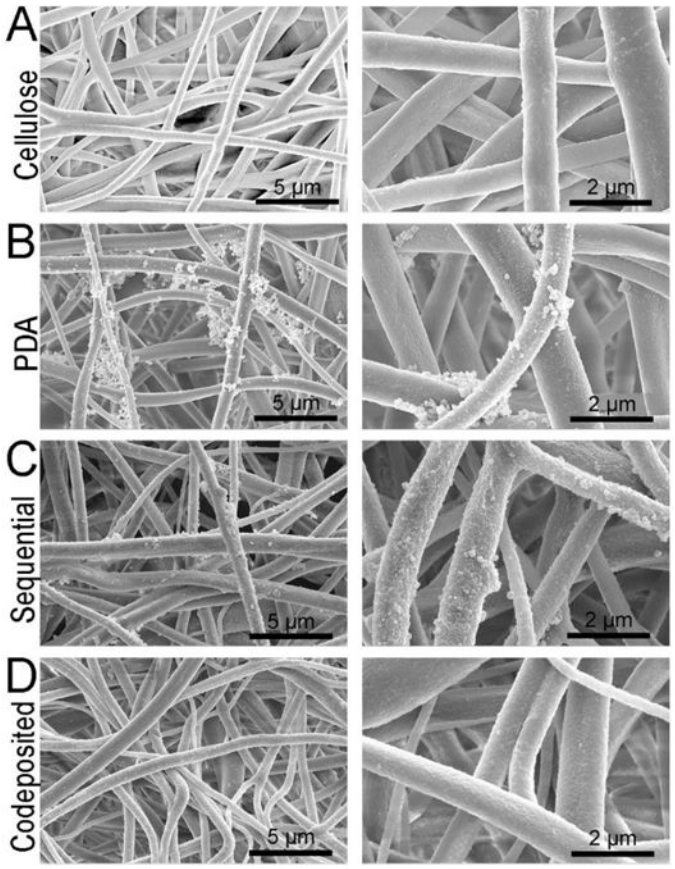

Figure 1.

(A) SEM micrographs of the cellulose nanofiber mats used as the base materials for this study. The morphology of **(B)** PDA and **(C, D)** polyMPC/PDA (sequential and codeposited) functionalized nanofiber mats are also displayed.

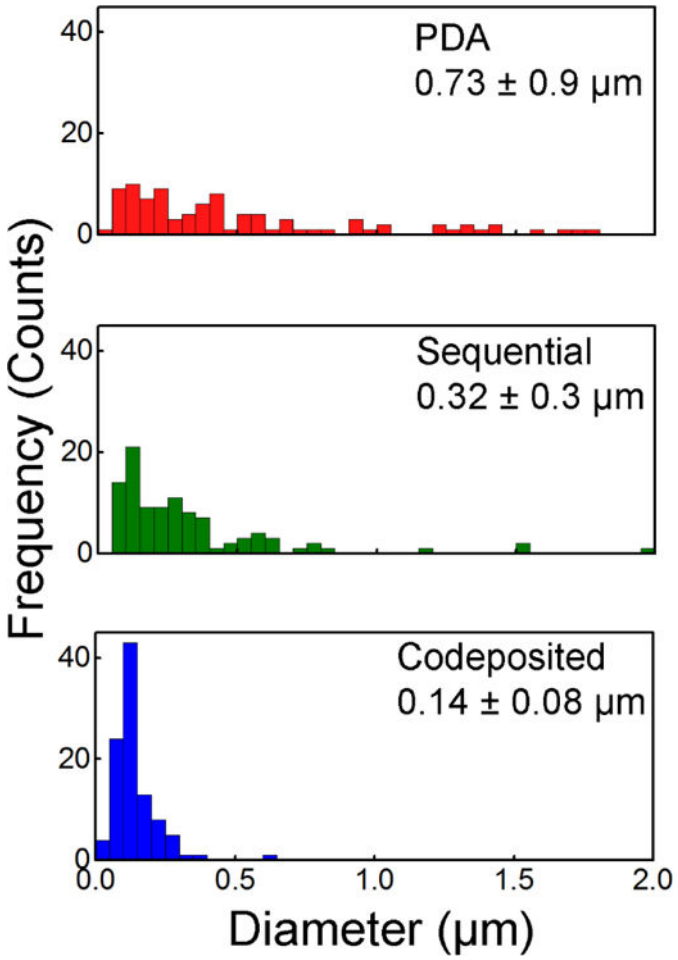

Figure 2.

Distribution of particle aggregate size on the PDA and polyMPC/PDA (sequential and codeposited) functionalized nanofiber surface are displayed along with their average size and standard deviation (n = 100).

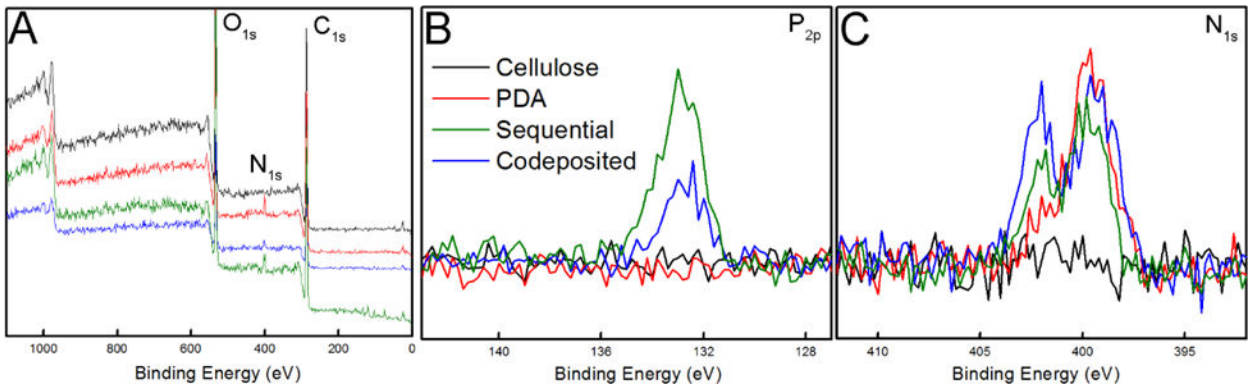

Figure 3.

XPS spectra of cellulose, PDA, and polyMPC/PDA (sequential and codeposited) functionalized nanofiber mats including **(A)** survey scans and **(B)** high resolution scans of P_{2p} and **(C)** N_{1s} as a function of electron binding energy.

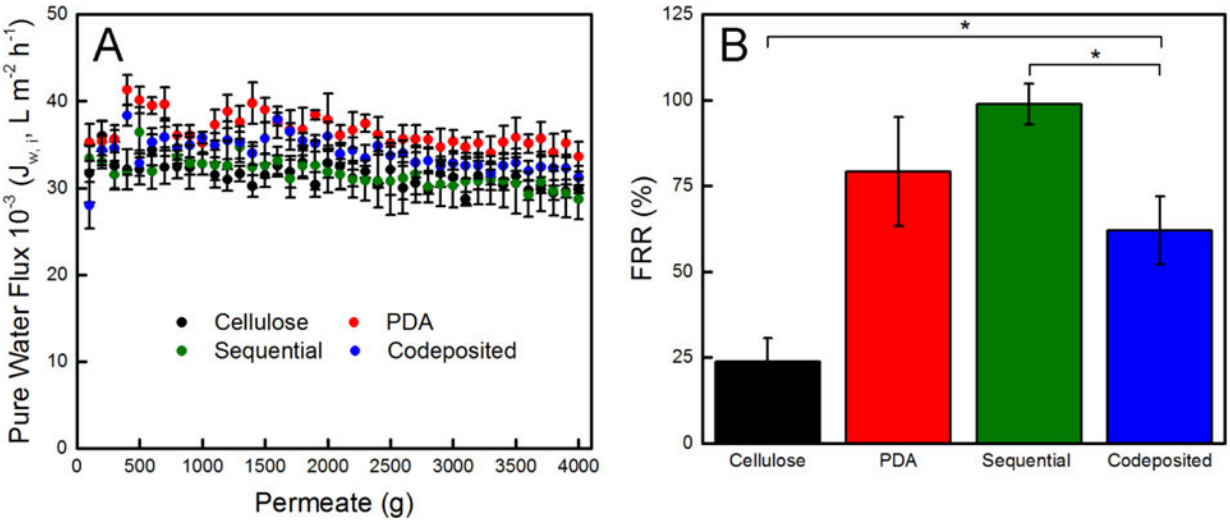

Figure 4.

(**A)** Pure water flux and **(B)** flux recovery ratio (FRR) of free-standing cellulose, PDA, and polyMPC/PDA (sequential and codeposited) functionalized nanofiber mats. Error bars denote standard error and one asterisk (*) denotes $P \leq 0.01$ significance between samples.

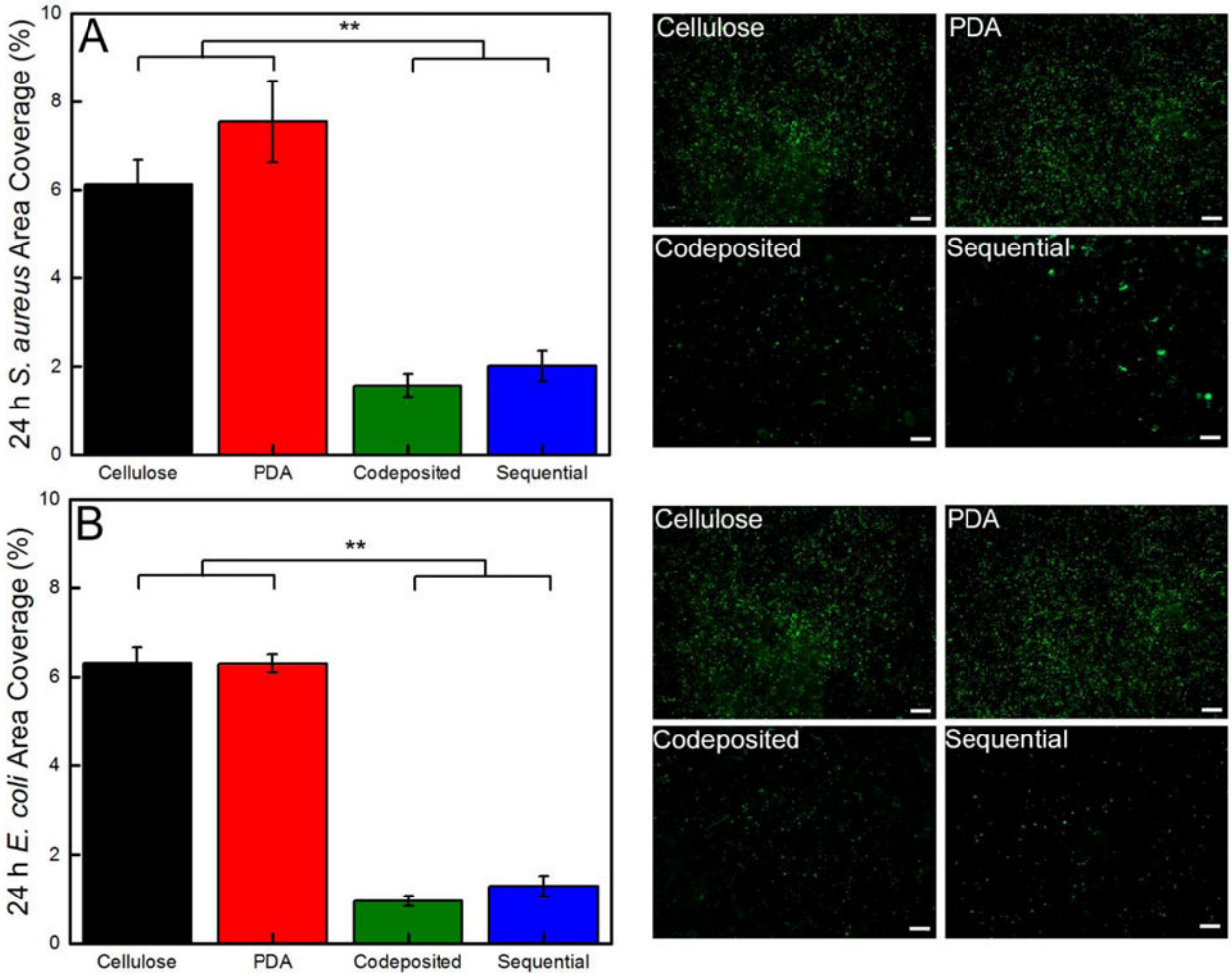

Figure 5.

Quantification of the area coverage of **(A)** *S. aureus* and (**B)** *E. coli* on the cellulose, PDA, and polyMPC/PDA (sequential and codeposited) functionalized nanofiber mats. Representative florescent micrographs (366964 μm^2) are also provided and a 50 μm scale bar is displayed. Error bars denote standard error and two asterisks (**) denotes $P \leq 0.001$ significance between samples.

Table 1

Summary of the elemental analysis of the high resolution XPS that provides composition analysis of cellulose, PDA, and polyMPC/PDA (sequential and codeposited) functionalized nanofiber mats.

Nanofiber Mat	C (%)	O (%)	N (%)	P (%)	O/C	N/C	P/C	N_{401}/N_{399}
Cellulose	58 ± 0.4	41 ± 0	0.7 ± 0.4	0.0	0.71	0.01	0.0	0.0
PDA	61 ± 1.8	37 ± 2.4	2.6 ± 0.8	0.0	0.6	0.04	0.002	0.0
Sequential	62 ± 1.4	34 ± 1.8	3.8 ± 1.0	0.8 ± 1.0	0.55	0.06	0.007	0.43 ± 0.2
Codeposited	61 ± 0.7	36 ± 0.4	2.7 ± 0.8	0.6 ± 0.2	0.59	0.04	0.01	0.36 ± 0.1